AIAA 95-3499

Determining the Accuracy of Aerodynamic Model Parameters Estimated from Flight Test Data

Eugene A. Morelli
Lockheed Engineering and Sciences Company
NASA Langley Research Center
Hampton, VA

Vladislav Klein
The George Washington University
NASA Langley Research Center
Hampton, VA

AIAA Atmospheric Flight Mechanics Conference
August 7 - 9, 1995 / Baltimore, MD

DETERMINING THE ACCURACY OF AERODYNAMIC MODEL PARAMETERS ESTIMATED FROM FLIGHT TEST DATA

Eugene A. Morelli*
Lockheed Engineering and Sciences Co.
NASA Langley Research Center
Hampton, Virginia

Vladislav Klein†
The George Washington University
NASA Langley Research Center
Hampton, Virginia

Abstract

An important part of building mathematical models based on measured data is calculating the accuracy associated with statistical estimates of the model parameters. Indeed, without some idea of this accuracy, the parameter estimates themselves have limited value. In this work, an expression for computing quantitatively correct parameter accuracy measures for maximum likelihood parameter estimates with colored residuals is developed and validated. This result is important because experience in analyzing flight test data reveals that the output residuals from maximum likelihood estimation are almost always colored. The calculations involved can be appended to conventional maximum likelihood estimation algorithms. Monte Carlo simulation runs were used to show that parameter accuracy measures from the new technique accurately reflect the quality of the parameter estimates from maximum likelihood estimation without the need for correction factors or frequency domain analysis of the output residuals. The technique was applied to flight test data from repeated maneuvers flown on the F-18 High Alpha Research Vehicle (HARV). As in the simulated cases, parameter accuracy measures from the new technique were in agreement with the scatter in the parameter estimates from repeated maneuvers, while conventional parameter accuracy measures were optimistic.

Nomenclature

a_z	vertical acceleration, g units
$\bar{c}$	mean aerodynamic chord, ft
C_L	lift coefficient
$\mathbf{D}$	dispersion matrix
$E\{\cdot\}$	expected value
g	gravitational acceleration, 32.174 ft/sec^2
I_{yy}	pitch axis moment of inertia, slug-ft^2
J	cost function
m	mass, slugs
$\mathbf{M}$	information matrix
n_o	number of outputs
n_p	number of parameters
N	total number of sample times
q	body axis pitch rate, rad/sec
$\bar{q}$	dynamic pressure, lbf/ft^2
$\mathbf{R}$	discrete noise covariance matrix
$\mathfrak{R}_{\mathbf{vv}}$	autocorrelation matrix of vector $\mathbf{v}$
s	sample standard error
S	wing area, ft^2
$\mathbf{S}(i)$	output sensitivity matrix at time $(i-1)\Delta t$
t	time, sec
$\mathbf{u}(t)$	control vector
V	airspeed, ft/sec
$\mathbf{v}(i)$	output residual vector at time $(i-1)\Delta t$
$\mathbf{x}(t)$	state vector
$\mathbf{y}(t)$	output vector
$\mathbf{z}(i)$	measured output at time $(i-1)\Delta t$
α	angle of attack, rad
δ_{ij}	Kronecker delta
δ_s	stabilator deflection, rad
Δt	sample time, sec
Φ	roll angle, rad
Θ	pitch angle, rad
$\boldsymbol{\theta}$	parameter vector
$\nabla_{\boldsymbol{\theta}}$	gradient with respect to $\boldsymbol{\theta}$
θ	element of the parameter vector
σ	Cramér-Rao bound for the standard error of $\hat{\theta}$
$\mathbf{v}(i)$	noise vector at time $(i-1)\Delta t$
$\mathbf{0}$	zero vector
$\forall$	for every

* Principal Research Engineer, Senior Member AIAA

† Professor, Associate Fellow AIAA

superscripts

T	transpose
$\hat{}$	estimate
$\bar{}$	mean value
$\dot{}$	time derivative
-1	matrix inverse

subscripts

m	measured
o	initial
c	corrected
w	wind axes

Introduction

Aircraft dynamic models typically include parameters which quantify the dependence of aerodynamic forces and moments on state and control variables. The values of these parameters are often estimated from flight test data. A good quantitative assessment of the accuracy of these parameter estimates is important for a variety of reasons related to experiment design, modeling, simulation, and flight control.

Maximum likelihood[1] is commonly used to estimate aerodynamic parameters from flight test data. Assuming the model structure is correct, maximum likelihood parameter estimates approach the true parameter values, and the parameter variances approach their theoretical minimum values (the Cramér-Rao lower bounds), as the number of measured data points increases. Generally, a flight test data record length at least 2-3 times the period of the slowest dynamic mode to be modeled is sufficient for the parameter biases to be small and for the parameter variances to closely approach the Cramér-Rao bounds[2]. In such cases, the Cramér-Rao bound can be used as a good approximation to the variance of maximum likelihood parameter estimates. References [2]-[4] compare and contrast the Cramér-Rao bound with other methods for assessing the accuracy of parameter estimates. Theoretical properties of maximum likelihood estimators and related arguments discussed in reference [2] indicate that the Cramér-Rao bound is the best accuracy measure for maximum likelihood parameter estimates.

The research described here focuses on the output error formulation of maximum likelihood parameter estimation. This formulation includes measurement noise, but no process noise[1]. A modified Newton-Raphson optimization procedure[1,5] was used to determine the maximum likelihood parameter estimates. With this approach, the Cramér-Rao bounds are computed as part of the estimation procedure. It is well known, however, that the Cramér-Rao bounds computed in this way are usually optimistic (too small) compared to the scatter in the parameter estimates from repeated flight test maneuvers[2,6]. This prompted the work of Maine, Iliff and Balakrishnan[1,2,7-9], who traced the discrepancy to the fact that the residuals are colored for real flight test data analysis because some deterministic modeling error is always present. Output error techniques lump the deterministic modeling error together with the broad band random part of a measured signal and call this the measurement noise. This means the measurement noise is model-dependent and colored, because the modeling error usually lies in the same frequency band as the aircraft rigid body dynamics and accounts for a large part of the total noise power. References [1],[2],[7]-[9] describe how this kind of colored measurement noise is responsible for the discrepancy between the conventional calculation of the Cramér-Rao bounds and the observed scatter in flight-determined parameter estimates from repeated maneuvers.

The theory underlying the output error formulation of maximum likelihood estimation assumes that the measurement noise is white Gaussian and band limited by the Nyquist frequency. The band limit is the result of discrete measurements taken at the sampling frequency, which is twice the Nyquist frequency. This measurement noise is broad band and incoherent. The term incoherent implies amplitude discontinuity and a lack of consistent phase-amplitude relationships, causing the autocorrelation function to be close to the impulse function. This part of the residual would be commonly recognized as having no deterministic component. If the structure of the model were correct, the residuals would be expected to be reasonably close to this type of noise. In real flight test data analysis, however, the residuals contain deterministic components from such sources as approximations to real aircraft aerodynamic dependencies, unmodeled dynamics such as structural modes, and linearization of the nonlinear equations of motion. The result is colored residuals which violate the assumptions of conventional maximum likelihood theory and lead to the aforementioned discrepancy[1,2,7-9].

In reference [2], several engineering solutions were proposed to correct for the discrepancy. Each solution was based on the assumption that most of the residual power for real flight data analysis is concentrated in roughly the same frequency band as the rigid body dynamics and is due to deterministic modeling error. This assumption is stretched when relatively high frequency structural modes appear in the data or when the broad band random noise has a large enough magnitude to rival the power of the narrow band noise due to modeling error. For multiple outputs, the noise power from broad band random noise compared to that from narrow band deterministic modeling error is different for each output because of differences in the sensor characteristics and the physical quantity being measured. The solutions offered in reference [2] depend on knowing something about the bandwidth of the dominant source of power in the residuals. Obtaining this information requires Fourier transforms of the residuals and analysis in the frequency domain. The spectra of the

residuals depend on the model structure, the maneuver, the flight condition, and the instrumentation characteristics. All of these factors can change over the course of a flight test program, requiring changes in the corrections for the Cramér-Rao bounds. In addition, the bandwidths of the deterministic modeling error for the various measured outputs can be different from one another for the same maneuver. The solutions from reference [2] require some engineering judgment in the form of determining a correction factor or estimating the bandwidth of the dominant power in the residuals. Both of these approaches require an experienced analyst and limit the quantitative accuracy of the results.

In the present work, a technique first put forth in reference [10] was used to process the residuals of a conventional maximum likelihood estimation in order to compute quantitatively accurate Cramér-Rao lower bounds for colored residuals. The approach accounts for colored residuals using a simple estimate of the residual correlation in the time domain. Existing maximum likelihood estimation routines can be easily upgraded because the technique involves a post-processing of the output residuals to correct the Cramér-Rao lower bounds from the conventional calculation. The purpose of the present work is to document a few refinements to the technique described in reference [10], to validate the technique using Monte Carlo simulation with colored measurement noise, and to apply the technique to real data from repeated flight test maneuvers.

The next section contains the theoretical analysis. Following this, the technique was applied in a controlled situation using simulated data from a model of the longitudinal dynamics of a fighter aircraft. The true parameter values were known, and the measured outputs were corrupted with colored noise, including both narrow band modeling error and broad band random noise. Using 200 Monte Carlo simulation runs with various colored noise characteristics, it was demonstrated that the new technique produces Cramér-Rao bounds representative of the observed scatter in the estimates. The conventional Cramér-Rao bounds were found to be optimistic, in agreement with the results of previous research[1,2,6-9].

Next, the technique was applied to repeated longitudinal flight test maneuvers at 20 deg angle of attack for the F-18 High Alpha Research Vehicle (HARV) aircraft. The scatter in the model parameter estimates from this flight test data was consistent with the Cramér-Rao bounds computed using the new technique, while the conventional calculation again gave optimistic values for the Cramér-Rao bounds.

Theoretical Development

The aircraft dynamic model can be represented as

$$\dot{\mathbf{x}}(t) = f(\mathbf{x}(t), \mathbf{u}(t), \boldsymbol{\theta}) \tag{1}$$

$$\mathbf{x}(0) = \mathbf{x}_o \tag{2}$$

$$\mathbf{y}(t) = g(\mathbf{x}(t), \mathbf{u}(t), \boldsymbol{\theta}) \tag{3}$$

$$\mathbf{z}(i) = \mathbf{y}(i) + \boldsymbol{\upsilon}(i) \qquad i = 1, 2, \ldots, N \tag{4}$$

The notation $\mathbf{y}(i)$ represents the sampled value of $\mathbf{y}(t)$ at $t = (i-1)\Delta t$. There are N sampled data points. For conventional maximum likelihood, the discrete measurement noise vector $\boldsymbol{\upsilon}(i)$ is assumed to be zero mean white Gaussian and band limited at the Nyquist frequency,

$$E\{\boldsymbol{\upsilon}(i)\} = \mathbf{0} \qquad E\{\boldsymbol{\upsilon}(i)\boldsymbol{\upsilon}^T(j)\} = \mathbf{R}\,\delta_{ij} \tag{5}$$

The maximum likelihood estimate of the parameter vector maximizes the conditional probability of realizing the measurements[1,5]:

$$\hat{\boldsymbol{\theta}} = arg \max_{\boldsymbol{\theta}} \left[P(\mathbf{Z} \mid \boldsymbol{\theta}) \right] \tag{6}$$

where $\mathbf{Z}$ is the set of all measurement vectors $\mathbf{z}(i)$, for i=1, 2, ..., N. The conditional probability distribution, $P(\mathbf{Z} \mid \boldsymbol{\theta})$, also known as the likelihood function, is given by

$$P(\mathbf{Z} \mid \boldsymbol{\theta}) = \left[(2\pi)^{n_o} |\mathbf{R}| \right]^{-N/2} \cdot exp\left\{ -\frac{1}{2} \sum_{i=1}^{N} [\mathbf{z}(i) - \mathbf{y}(i)]^T \mathbf{R}^{-1} [\mathbf{z}(i) - \mathbf{y}(i)] \right\} \tag{7}$$

Maximizing the likelihood function in Eq. (7) is equivalent to minimizing its negative logarithm, known as the log likelihood function,

$$-\ln\left[P(\mathbf{Z} \mid \boldsymbol{\theta})\right] = \frac{1}{2} \sum_{i=1}^{N} [\mathbf{z}(i) - \mathbf{y}(i)]^T \mathbf{R}^{-1} [\mathbf{z}(i) - \mathbf{y}(i)] + \frac{N}{2} \ln|\mathbf{R}| \tag{8}$$

where the added constant $\frac{n_o N}{2}\ln(2\pi)$ was omitted because it has no effect on the optimization. When $\mathbf{R}$ is known, minimizing the log likelihood function in Eq. (8) is equivalent to minimizing the cost function

$$J(\boldsymbol{\theta}) = \frac{1}{2}\sum_{i=1}^{N}\left[\mathbf{z}(i)-\mathbf{y}(i)\right]^T \mathbf{R}^{-1}\left[\mathbf{z}(i)-\mathbf{y}(i)\right] \qquad (9)$$

The cost in Eq. (9) can be minimized using a modified Newton-Raphson technique to determine parameter updates[1,5], starting from some initial guess of the parameter vector. The initial guess for the parameter vector can be obtained from equation error methods[6]. Define the sensitivity matrix

$$\mathbf{S}(i) \equiv \left.\frac{\partial \mathbf{y}(i)}{\partial \boldsymbol{\theta}}\right|_{\boldsymbol{\theta}=\hat{\boldsymbol{\theta}}} \qquad i = 1,2,\ldots,N \quad (10)$$

where the jth column of the sensitivity matrix contains the output sensitivities for the jth parameter, computed from central finite differences in Eqs. (1)-(3). The modified Newton-Raphson parameter update is given by[1,5,10]

$$\Delta\hat{\boldsymbol{\theta}} \equiv \boldsymbol{\theta} - \hat{\boldsymbol{\theta}} = \left[\sum_{i=1}^{N}\mathbf{S}(i)^T\mathbf{R}^{-1}\mathbf{S}(i)\right]^{-1}\sum_{i=1}^{N}\mathbf{S}(i)^T\mathbf{R}^{-1}\left[\mathbf{z}(i)-\hat{\mathbf{y}}(i)\right] \qquad (11)$$

The parameter vector update from Eq. (11) is added to the current estimate of the parameter vector in order to approach the true value of the parameter vector. In practice, there are times when the parameter vector update computed from Eq. (11) leads to an increase in the cost function or a divergence. This is because the modified Newton-Raphson step assumes that the current estimate of the parameter vector is near the true value. Using several iterations of a simplex algorithm[11] when the modified Newton-Raphson step produced an increase in the cost was found to be very effective in avoiding divergence and reaching a solution. This approach was followed in the present study.

When repeated application of Eq. (11) converges, an estimate of the measurement noise covariance matrix, $\mathbf{R}$, can be obtained from the output residuals. The expression for the estimate of $\mathbf{R}$ comes from taking the derivative of the right hand side of Eq. (8) with respect to $\mathbf{R}$, setting the result equal to zero, and solving for $\mathbf{R}$,

$$\hat{\mathbf{R}} = \frac{1}{N}\sum_{i=1}^{N}\left[\mathbf{z}(i)-\mathbf{y}(i)\right]\left[\mathbf{z}(i)-\mathbf{y}(i)\right]^T \qquad (12)$$

Often only the diagonal elements of the $\mathbf{R}$ matrix are estimated from Eq. (12), enforcing an assumption that the measurement noise sequences for the measured outputs are uncorrelated with one another. This assumption is generally a good one for real flight test data. All estimates of the measurement noise covariance matrix in this work assume a diagonal $\hat{\mathbf{R}}$ matrix. Retaining the full $\hat{\mathbf{R}}$ matrix could have been done with little conceptual difficulty, but the expected gains did not warrant the extra computation involved. The noise covariance matrix estimate, $\hat{\mathbf{R}}$, was used in the cost function of Eq. (9), and the minimization process described above for known $\mathbf{R}$ was repeated. Thus, the maximum likelihood estimation proceeds by alternately estimating the noise covariance matrix from Eq. (12) and minimizing the cost function using Eq. (11) with the latest value of the estimated noise covariance matrix. Convergence is reached when the estimated parameter vector $\hat{\boldsymbol{\theta}}$, the estimated noise covariance matrix $\hat{\mathbf{R}}$, and the cost $J(\hat{\boldsymbol{\theta}})$ reach nearly constant values. Since maximum likelihood estimation is asymptotically unbiased[1,2], the estimated parameter vector $\hat{\boldsymbol{\theta}}$ should be close to the true value $\boldsymbol{\theta}$, and the gradient of the cost function with respect to the parameter vector should be close to zero. From Eq. (9), assuming $\mathbf{R}$ is held fixed,

$$\nabla_{\boldsymbol{\theta}} J(\boldsymbol{\theta})\big|_{\boldsymbol{\theta}=\hat{\boldsymbol{\theta}}} \approx -\sum_{i=1}^{N}\mathbf{S}(i)^T\mathbf{R}^{-1}\left[\mathbf{z}(i)-\hat{\mathbf{y}}(i)\right] \qquad (13)$$

For practical computation, simultaneous satisfaction of the numerical criteria given below were used to define convergence of the maximum likelihood estimation:

$$\begin{aligned}
&\left|\left[\hat{\theta}_j\right]_k - \left[\hat{\theta}_j\right]_{k-1}\right| < 1.0 \times 10^{-5} \quad \forall\, j, \quad j = 1,2,\ldots,n_p \\
&\left|\frac{\left[\hat{r}_{ii}\right]_k - \left[\hat{r}_{ii}\right]_{k-1}}{\left[\hat{r}_{ii}\right]_{k-1}}\right| < 0.05 \quad \forall\, i, \quad i = 1,2,\ldots,n_o \\
&\left|\frac{J(\hat{\boldsymbol{\theta}}_k) - J(\hat{\boldsymbol{\theta}}_{k-1})}{J(\hat{\boldsymbol{\theta}}_{k-1})}\right| < 0.001 \\
&\left|\frac{\partial J(\boldsymbol{\theta})}{\partial \theta_j}\right|_{\boldsymbol{\theta}=\hat{\boldsymbol{\theta}}} < 0.05 \quad \forall\, j, \quad j = 1,2,\ldots,n_p
\end{aligned} \qquad (14)$$

where k denotes the current estimate iteration number and $\hat{r}_{ii}$ denotes the estimate of the ith diagonal element of $\mathbf{R}$. The approximate expression for the cost gradient with respect to the parameters (Eq. (13)) was used for the last criterion in (14).

The minimum achievable parameter variances, the Cramér-Rao lower bounds, are given by the diagonal

elements of the dispersion matrix, **D** [1,2,5]. This dispersion matrix is defined as the inverse of the information matrix **M**, the latter being a measure of the information contained in the data from an experiment. The expressions for these matrices are[1,2,5]

$$\mathbf{M} = \sum_{i=1}^{N} \mathbf{S}(i)^T \mathbf{R}^{-1} \mathbf{S}(i) \tag{15}$$

$$\mathbf{D} = \mathbf{M}^{-1} = \left[\sum_{i=1}^{N} \mathbf{S}(i)^T \mathbf{R}^{-1} \mathbf{S}(i) \right]^{-1} \tag{16}$$

The square root of the jth diagonal element of **D**, d_{jj}, gives the Cramér-Rao lower bound for the standard error of the jth parameter estimate,

$$\sigma_j = \sqrt{d_{jj}} \qquad j = 1, 2, \ldots, n_p \tag{17}$$

It can be seen from Eqs. (11) and (16) that the dispersion matrix is computed when determining the modified Newton-Raphson step as part of the conventional maximum likelihood estimation . The assumption that the output residuals are white and therefore uncorrelated in time is implicit in the algorithm and indicated in Eq. (5). The next section details the theory involved in accounting for arbitrary colored output residuals, which are correlated in time.

When the conventional maximum likelihood estimation has converged, the estimated parameter vector will be close to the true value and Eq. (11) holds. Define the residual vector

$$\mathbf{v}(i) \equiv \mathbf{z}(i) - \hat{\mathbf{y}}(i) \qquad i = 1, 2, \ldots, N \tag{18}$$

The estimated parameter covariance matrix can be expressed using Eq. (11) with substitutions from the definitions in Eqs. (16) and (18),

$$cov\left(\hat{\boldsymbol{\theta}}\right) \equiv E\left\{ \left(\hat{\boldsymbol{\theta}} - \boldsymbol{\theta}\right)\left(\hat{\boldsymbol{\theta}} - \boldsymbol{\theta}\right)^T \right\}$$

$$= E\left\{ \sum_{i=1}^{N} \sum_{j=1}^{N} \mathbf{D}\, \mathbf{S}(i)^T \mathbf{R}^{-1}\, \mathbf{v}(i)\mathbf{v}(j)^T \mathbf{R}^{-1} \mathbf{S}(j)\, \mathbf{D} \right\} \tag{19}$$

If it is assumed that the discrete noise covariance matrix and the output sensitivities do not depend on the parameter vector estimate at the maximum likelihood solution, then the estimated parameter covariance matrix can be written as

$$cov\left(\hat{\boldsymbol{\theta}}\right) = \mathbf{D} \left[\sum_{i=1}^{N} \sum_{j=1}^{N} \mathbf{S}(i)^T \mathbf{R}^{-1} E\left\{ \mathbf{v}(i)\mathbf{v}(j)^T \right\} \mathbf{R}^{-1} \mathbf{S}(j) \right] \mathbf{D} \tag{20}$$

When the output residuals are assumed to be zero mean white (cf Eq. (5)), then

$$E\left\{ \mathbf{v}(i)\mathbf{v}(j)^T \right\} = \mathbf{R}\,\delta_{ij} \tag{21}$$

From Eqs. (16), (20) and (21) it is easy to see that the parameter covariance matrix reduces to the dispersion matrix **D** when the output residuals are white.

For colored residuals,

$$E\left\{ \mathbf{v}(i)\mathbf{v}(j)^T \right\} = \mathfrak{R}_{\mathbf{vv}}(i-j) \tag{22}$$

where $\mathfrak{R}_{\mathbf{vv}}(i-j)$ is the autocorrelation of the output residuals, so that the estimated parameter covariance matrix can be computed from Eq. (20) using an estimated value for $\mathfrak{R}_{\mathbf{vv}}(i-j)$. Define the discrete unbiased estimate of the output residual autocorrelation[12]

$$\hat{\mathfrak{R}}_{\mathbf{vv}}(k) \equiv \frac{1}{N-k} \sum_{i=1}^{N-k} \mathbf{v}(i)\mathbf{v}(i+k)^T = \hat{\mathfrak{R}}_{\mathbf{vv}}(-k) \tag{23}$$

Substituting Eq. (22) into Eq. (20) results in

$$cov\left(\hat{\boldsymbol{\theta}}\right) = \mathbf{D} \left[\sum_{i=1}^{N} \mathbf{S}(i)^T \mathbf{R}^{-1} \sum_{j=1}^{N} \mathfrak{R}_{\mathbf{vv}}(i-j)\, \mathbf{R}^{-1} \mathbf{S}(j) \right] \mathbf{D} \tag{24}$$

Eq. (24) was used to account for colored residuals, which are correlated in time. Eq. (23) was used to estimate $\mathfrak{R}_{\mathbf{vv}}(i-j)$ in Eq. (24). The values for **D**, $\mathbf{R}^{-1}$, and **S** are from the conventional maximum likelihood estimation. Eqs. (23) and (24) embody the post-processing applied to a conventional maximum likelihood solution to account for colored residuals.

If the colored output residuals are assumed to be caused by modeling error, then the maximum likelihood parameter estimates are biased, so that

$$E\left\{ \hat{\boldsymbol{\theta}} \right\} = \boldsymbol{\theta} + \mathbf{b}(\boldsymbol{\theta}) \tag{25}$$

where $\mathbf{b}(\boldsymbol{\theta})$ is a vector of bias errors which are unknown and unknowable in practice. For these biased parameter estimates, the Cramér-Rao bound will contain terms in

addition to $\mathbf{D}$, namely $\mathbf{D}$ multiplied by $\nabla_{\boldsymbol{\theta}}\mathbf{b}(\boldsymbol{\theta})$ and $[\nabla_{\boldsymbol{\theta}}\mathbf{b}(\boldsymbol{\theta})][\nabla_{\boldsymbol{\theta}}\mathbf{b}(\boldsymbol{\theta})]^T$ (see reference [2] for details). In the present analysis, the deterministic modeling error is included as part of the measurement noise, making the residuals colored. The approach taken here for arbitrary frequency content in the measurement noise could then be viewed as effectively including the bias error due to deterministic modeling error as part of the parameter accuracy measure that accounts for colored residuals.

Results

The longitudinal short period dynamics of the F-18 HARV fighter aircraft at approximately 20 degrees angle of attack were studied. The model state equations in wind axes are given by

$$\dot{\alpha} = \frac{\bar{q}S}{mV}\left(C_{Z_\alpha}\alpha + C_{Z_q}\frac{q\bar{c}}{2V} + C_{Z_{\delta_s}}\delta_s\right) + q + \frac{g}{V}\left(\cos(\Phi_m)\cos(\Theta_m)\cos(\alpha) + \sin(\Theta_m)\sin(\alpha)\right) + \dot{\alpha}_o^*$$

$$\dot{q} = \frac{\bar{q}S\bar{c}}{I_{yy}}\left(C_{M_\alpha}\alpha + C_{M_q}\frac{q\bar{c}}{2V} + C_{M_{\delta_s}}\delta_s\right) + \dot{q}_o^* \tag{26}$$

with measurement equations

$$\alpha_m(i) = \alpha(i) + v_1(i)$$

$$q_m(i) = q(i) + v_2(i)$$

$$a_{z_m}(i) = \frac{\bar{q}S}{mg}\left(C_{Z_\alpha}\alpha(i) + C_{Z_q}\frac{q(i)\bar{c}}{2V} + C_{Z_{\delta_s}}\delta_s(i)\right) + a_{z_o} + v_3(i) \qquad i = 1, 2, \ldots, N \tag{27}$$

assuming that $C_Z \approx -C_L$, $a_{z_w} \approx a_z$, and where $\dot{\alpha}_o^* \equiv (\bar{q}S/mV)C_{Z_o} + \dot{\alpha}_o$ and $\dot{q}_o^* \equiv (\bar{q}S\bar{c}/I_{yy})C_{M_o} + \dot{q}_o$. Initial conditions for the states were computed from the measured time histories of α and q using a time domain smoother[13].

To validate the new technique for computing Cramér-Rao bounds, two hundred Monte Carlo simulation runs were made using various colored measurement noise processes. Each noise sequence had part of its power in the frequencies between 0 hz and 1 hz inclusive (roughly the frequency band of the uncorrupted simulation outputs), with the remaining power taken up by white Gaussian noise out to the Nyquist frequency. The narrow band portion of the colored noise sequence was generated by passing zero mean white Gaussian noise through a fifth order Chebyshev low pass filter with frequency cutoff set at 1 hz. The resulting narrow band noise was combined with wide band noise from a separate realization of the zero mean white Gaussian noise process. The percentage of the total noise power from the narrow band noise was determined for each Monte Carlo run by a random number with uniform distribution on the interval [0,100]. This procedure was carried out for each simulated output on each Monte Carlo run, and the resulting colored noise sequences were scaled to achieve approximately a 5 to 1 signal to noise ratio for all simulated outputs. Figure 1 shows the power spectral density for the colored noise added to α for run 200, where 19% of the noise power was in the frequency range of 0 hz to 1 hz, inclusive. Colored noise sequences generated in this way are representative of residual sequences observed when analyzing real flight test data, and were used for that reason.

To make the Monte Carlo simulation runs realistic, the stabilator input was taken from measured data for the F-18 HARV flying a maneuver designed specifically for accurate parameter estimation[14]. The stabilator input is shown as the solid line in figure 2. The values of the parameters used in the simulations (given in column 2 of Table 1) approximately reflect the short period dynamics of the F-18 HARV at 20 degrees angle of attack. The stabilator input and parameter values were the same for each simulated data run, so that the information in the data was constant. The sampling rate was 50 hz and the data record length was 14 seconds. Maximum likelihood estimation as described in the previous section was used to estimate the parameters.

Since the parameter values were known for the simulated data, the true accuracy of the maximum likelihood estimates could be compared to the accuracy indicated by the Cramér-Rao bound calculations. The conventional Cramér-Rao bounds for the parameter standard errors were denoted by σ and were computed as the square root of the diagonal elements of matrix $\mathbf{D}$ in Eq. (16). The Cramér-Rao bounds for the parameter standard errors corrected for colored residuals were denoted by σ_c and were computed as the square root of the diagonal elements of the covariance matrix from Eq. (24). Results from both the conventional computation and the corrected calculation were expressed in terms of the ratio of the absolute deviation of each parameter estimate from its true value to the computed Cramér-Rao bound for the parameter standard error. This accuracy measure was assigned the symbol η,

$$\eta \equiv \left|\hat{\theta} - \theta\right| / \sigma$$

$$\eta_c \equiv \left|\hat{\theta} - \theta\right| / \sigma_c \tag{28}$$

where the subscript c denotes values for the corrected Cramér-Rao bounds.

For a maximum likelihood estimator, the probability distribution of the parameter estimates about their true value

approaches a Gaussian distribution as the number of data points gets large. Evidence of this can be found in figure 3, which is a histogram of the parameter estimates from all two hundred Monte Carlo runs for the C_{M_α} parameter. Corresponding histograms for the other estimated parameters were similar. It follows that η and η_c should be less than 3 almost all the time if the computed Cramér-Rao bounds reflect the true accuracy of the parameter estimates.

Table 1 shows results for two representative Monte Carlo runs. Columns 4 and 5 for run 47 and columns 7 and 8 for run 185 show that the corrected Cramér-Rao bounds accurately reflected the true parameter accuracy, while the conventional Cramér-Rao bounds were optimistic (i.e., too small) and produced η ratios which exceeded 3 for almost every estimated parameter. Considering the full set of two hundred Monte Carlo runs, Table 2 gives the mean values and standard errors of η and η_c for each estimated parameter. This data shows that the conventional Cramér-Rao bounds were inaccurate on the average and exhibited a large variability, while the converse was true for the corrected Cramér-Rao bounds.

Table 3 gives another summary of the parameter estimation results for the two hundred Monte Carlo simulation runs. The second column of the table gives the mean values of the parameter estimates, and the third column gives the sample standard errors for the parameter estimates, s, computed from the scatter of the parameter estimates. Columns 4 and 6 give the mean values of the Cramér-Rao bounds for the parameter standard errors computed using the conventional and corrected techniques, $\overline{\sigma}$ and $\overline{\sigma}_c$, respectively. Columns 5 and 7 show the ratio of the sample standard errors for the parameter estimates to $\overline{\sigma}$ and $\overline{\sigma}_c$, respectively. These values are far less than 3 for the corrected calculation of the Cramér-Rao bounds, indicating a proper accounting for the changes in the residual spectra, while the conventional calculation of the Cramér-Rao bound was optimistic, producing values of the $s/\overline{\sigma}$ ratio greater than 3.

The data in Tables 1,2, and 3 demonstrate that the extent to which the conventional Cramér-Rao bounds misrepresented the true parameter accuracy was neither consistent nor predictable from parameter to parameter or from run to run. This phenomena has been observed previously when analyzing flight test data from repeated maneuvers[6]. It follows that the common practice of applying a fixed correction factor to the conventional calculation of the Cramér-Rao bounds is incorrect to a varying and unpredictable degree in cases where coloring of the residual spectrum varies, as in this simulation study. Changes in the coloring of the residuals similar to those studied here can easily be brought about in practice by changes in the model structure, the maneuver, the flight condition, or the instrumentation.

Next, flight test data was analyzed from five repeats of the same longitudinal maneuver, flown on the F-18 HARV at approximately 20 degrees angle of attack and 25,000 feet. The input was applied to the symmetric stabilator by a computerized On-Board Excitation System (OBES), so that the runs were very nearly repeats of one another. Figure 2 shows the excellent repeatability using the OBES system for the five repeated flight test runs of the stabilator input maneuver. All of the data used for analysis was sampled at 50 hz. Corrections were applied to the angle of attack and accelerometer measurements to account for sensor offsets from the center of gravity, and the angle of attack measurement was corrected for upwash. Data compatibility analysis[15] revealed that the data from the sensors was consistent to a degree which warranted no further corrections. Maximum likelihood estimation was carried out using the same procedure as for the Monte Carlo simulation runs. The same model given in Eqs. (26)-(27) was used.

Table 4 gives flight test results in a form similar to Table 3. Column 7 shows that the corrected Cramér-Rao bounds were an accurate measure of the scatter in the parameter estimates. In column 5, the conventional Cramér-Rao bounds were again optimistic for the pitching moment (C_M) parameters but were close to correct for the vertical force (C_Z) parameters. The reason is that the α and a_z measurements are the main influences on the C_Z parameters, and the residuals for both these outputs exhibited considerable power at high frequencies, due to unmodeled structural modes. The power spectrum for a typical a_z residual (from run 1) is shown in figure 4. These colored residual spectra roughly resembled constant power out to the Nyquist frequency, which is the assumption made in the theory underlying the conventional Cramér-Rao bound calculation. The q measurement did not have these high frequency components, so the conventional Cramér-Rao bound calculation gave very optimistic values for the C_M parameters. The power spectrum for a typical q residual (from run 1) is shown in figure 5. The corrected calculation of the Cramér-Rao bound worked equally well for the C_Z and C_M parameters because information about the particular coloring of the residuals is incorporated automatically via the autocorrelation estimate from Eq. (23) used in Eq. (24).

Figures 6 and 7 depict the parameter estimation results for the aerodynamic parameters. The error bars represent the Cramér-Rao bounds for the standard errors computed using the conventional calculation for figure 6 and the corrected calculation for figure 7. The error bars in the lower three plots of figure 6 are difficult to see because they are roughly the size of the circles on the plot marking the individual parameter estimates. These plots and the accompanying data in Table 4 show that the standard calculation for the Cramér-Rao bounds gave optimistic values compared to the scatter in the estimates from repeated maneuvers, whereas the corrected calculation for the Cramér-Rao bounds produced Cramér-Rao bounds which accurately reflected the scatter of the estimates.

Concluding Remarks

Algorithms for aircraft parameter estimation using the output error formulation of maximum likelihood are in widespread use. The Cramér-Rao bounds characterizing parameter accuracy that are obtained from conventional calculations are known to be generally optimistic (i.e., too small) in practice, compared to the scatter in parameter values estimated from repeated maneuvers. Parameter estimates have limited utility when there is no firm idea of their accuracy. In this work, an expression for correcting Cramér-Rao bounds from maximum likelihood estimation with colored residuals was presented and validated. This result is important because the residuals from maximum likelihood estimation are almost always colored in practice, due to deterministic modeling error.

The calculations involved in the algorithm for computing Cramér-Rao bounds that account for colored residuals can be carried out in a short subroutine called at the conclusion of a conventional maximum likelihood estimation algorithm. Bandwidth of the dominant power in the residuals need not be known or estimated, since it is accounted for automatically in the algorithm by an unbiased estimate of the residual autocorrelation. There is no need for correction factors. The algorithm was shown to work for a wide range of colored residual spectra similar to what might be encountered in real flight test data analysis. All calculations are performed in the time domain, obviating the need for frequency domain analysis of the residuals.

The corrected calculation for the Cramér-Rao bounds presented here produced consistently accurate measures of the scatter in the parameter estimates, using an algorithm with moderate computational cost that can be applied as a post-processing of the output residuals from a conventional maximum likelihood solution.

Monte Carlo simulation runs using various colored noise sequences were carried out to validate the performance of the algorithm. Analysis of flight data from repeated maneuvers flown on the F-18 High Alpha Research Vehicle (HARV) demonstrated the validity of the technique for computing appropriate parameter accuracy measures using real flight test data. The algorithm described in this work was shown to be an effective means of accurately determining the quality of parameter estimates from the output error formulation of maximum likelihood estimation.

Acknowledgments

This research was conducted at the NASA Langley Research Center under NASA contract NAS1-19000 and NASA cooperative agreement NCC1-29.

References

1. Maine, R.E. and Iliff, K.W., "Application of Parameter Estimation to Aircraft Stability and Control - The Output-Error Approach", NASA RP 1168, June 1986.

2. Maine, R.E. and Iliff, K.W., "The Theory and Practice of Estimating the Accuracy of Dynamic Flight-Determined Coefficients", NASA RP 1077, July 1981.

3. Murphy, P.C., "A Methodology for Airplane Parameter Estimation and Confidence Interval Determination in Nonlinear Estimation Problems", NASA RP 1153, April 1986.

4. Murphy, P.C., "Efficient Computation of Confidence Intervals of Parameters", AIAA paper 87-2624-CP, Atmospheric Flight Mechanics Conference, Monterey, California, August 1987 (also NASA Tech Brief LAR-14341).

5. Taylor, L.W., Jr. and Iliff, K.W. "Systems Identification using a Modified Newton-Raphson Method - A FORTRAN Program", NASA TN D-6734, May 1972.

6. Klein, V., "Determination of Stability and Control Parameters of a Light Airplane from Flight Data using Two Estimation Methods", NASA TP-1306, March 1979.

7. Iliff, K.W. and Maine, R.E., "Further Observations on Maximum Likelihood Estimates of Stability and Control Characteristics Obtained from Flight Data", AIAA paper 77-1133, Atmospheric Flight Mechanics Conference, Hollywood, Florida, August 1977.

8. Maine, R.E. and Iliff, K.W., "Use of Cramér-Rao Bounds on Flight Data with Colored Residuals", *Journal of Guidance and Control*, Vol. 4, No. 2, March-April 1981.

9. Balakrishnan, A.V. and Maine, R.E., "Improvements in Aircraft Extraction Programs", NASA CR 145090, 1975.

10. Morelli, E.A. and Klein, V., "Determining the Accuracy of Maximum Likelihood Parameter Estimates with Colored Residuals", NASA CR 194893, March 1994.

11. Press, W.H., Flannery, B.P., Teukolsky, S.A., and Vetterling, W.T. *Numerical Recipes (FORTRAN version)*, Cambridge University Press, New York, NY, 1989.

12. Bendat, J.S. and Piersol, A.G. *Random Data Analysis and Measurement Procedures*, 2nd Ed., John Wiley & Sons, New York, NY, 1986.

13. Graham, R.J., "Determination and Analysis of Numerical Smoothing Weights", NASA TR R-179, December 1963.

14. Morelli, E.A., "Practical Input Optimization for Aircraft Parameter Estimation Experiments", NASA CR 191462, May 1993.

15. Klein, V. and Morgan, D.R. "Estimation of Bias Errors in Measured Airplane Responses using Maximum Likelihood Method", NASA TM 89059, January 1987.

Table 1 PARAMETER ESTIMATION RESULTS FOR TYPICAL MONTE CARLO RUNS

		Run 47			Run 185		
	θ	$\hat{\theta}$	η	η_c	$\hat{\theta}$	η	η_c
C_{Z_α}	-2.00	-1.30	4.24	0.94	-3.78	9.33	2.26
C_{Z_q}	-65.0	-13.8	4.10	0.99	-81.8	1.37	0.33
$C_{Z_{\delta_s}}$	-0.90	-1.48	4.20	0.95	0.04	6.46	1.59
$\dot{\alpha}_o^*$	-0.80	-1.08	4.73	1.04	0.01	10.46	2.33
C_{M_α}	-0.30	-0.35	7.00	1.67	-0.32	3.09	0.48
C_{M_q}	-16.0	-17.3	3.55	0.86	-13.2	7.04	1.13
$C_{M_{\delta_s}}$	-0.70	-0.67	5.42	1.03	-0.72	3.86	0.57
$\dot{q}_o^*$	0.08	0.09	5.77	1.20	0.09	5.01	0.73
a_{z_o}	-0.70	-1.07	6.11	1.36	0.04	9.48	2.14

Table 2 PARAMETER ACCURACY MEASURE STATISTICS FOR 200 MONTE CARLO RUNS

	Conventional		Corrected	
	$\overline{\eta}$	σ_η	$\overline{\eta}_c$	σ_{η_c}
C_{Z_α}	3.84	2.85	1.37	1.10
C_{Z_q}	3.43	2.72	1.10	0.83
$C_{Z_{\delta_s}}$	3.30	2.51	1.10	0.91
$\dot{\alpha}_o^*$	3.88	2.89	1.36	1.05
C_{M_α}	4.03	3.42	1.44	1.38
C_{M_q}	3.62	2.66	1.26	1.08
$C_{M_{\delta_s}}$	3.63	2.72	1.23	0.88
$\dot{q}_o^*$	3.97	3.19	1.37	1.15
a_{z_o}	3.88	2.80	1.39	1.06

Table 3 PARAMETER ESTIMATION RESULTS FOR 200 MONTE CARLO RUNS

	Simulation		Conventional		Corrected	
	$\overline{\hat{\theta}}$	s	$\overline{\sigma}$	$s/\overline{\sigma}$	$\overline{\sigma}_c$	$s/\overline{\sigma}_c$
C_{Z_α}	-1.94	0.819	0.179	4.56	0.521	1.57
C_{Z_q}	-62.1	51.1	12.3	4.17	38.7	1.32
$C_{Z_{\delta_s}}$	-0.92	0.550	0.139	3.96	0.441	1.25
$\dot{\alpha}_o^*$	-0.82	0.312	0.068	4.56	0.199	1.57
C_{M_α}	-0.30	0.037	0.008	4.80	0.022	1.67
C_{M_q}	-16.1	1.822	0.448	4.07	1.278	1.43
$C_{M_{\delta_s}}$	-0.70	0.030	0.007	4.11	0.021	1.43
$\dot{q}_o^*$	0.08	0.013	0.003	4.67	0.008	1.64
a_{z_o}	-0.72	0.313	0.069	4.54	0.198	1.58

Table 4 PARAMETER ESTIMATION RESULTS FROM FLIGHT TEST DATA

	Flight		Conventional		Corrected	
	$\overline{\hat{\theta}}$	s	$\overline{\sigma}$	$s/\overline{\sigma}$	$\overline{\sigma}_c$	$s/\overline{\sigma}_c$
C_{Z_α}	-2.04	0.161	0.083	1.95	0.192	0.84
C_{Z_q}	-61.0	4.86	3.48	1.40	7.67	0.63
$C_{Z_{\delta_s}}$	-0.92	0.081	0.044	1.82	0.081	1.00
$\dot{\alpha}_o^*$	-0.72	0.068	0.031	2.21	0.068	1.00
C_{M_α}	-0.30	0.065	0.006	10.80	0.052	1.26
C_{M_q}	-19.1	2.55	0.372	6.86	2.84	0.90
$C_{M_{\delta_s}}$	-0.74	0.048	0.007	6.90	0.051	0.94
$\dot{q}_o^*$	0.08	0.025	0.002	10.62	0.020	1.24
a_{z_o}	-0.66	0.067	0.031	2.17	0.070	0.95

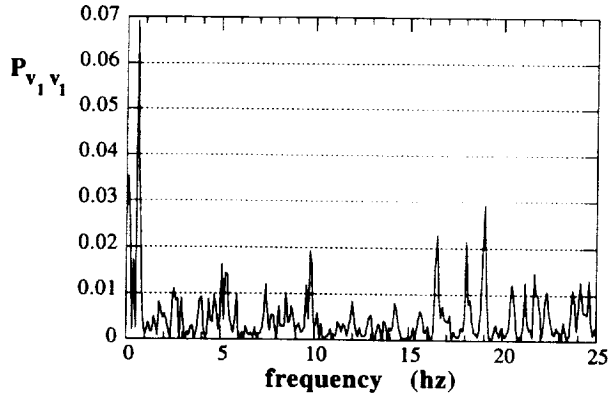

Figure 1 Example colored noise power spectrum, run 200

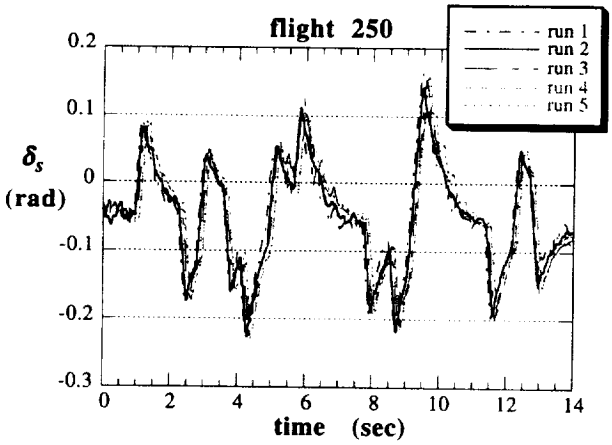

Figure 2 Stabilator input time histories from five repeated flight test maneuvers

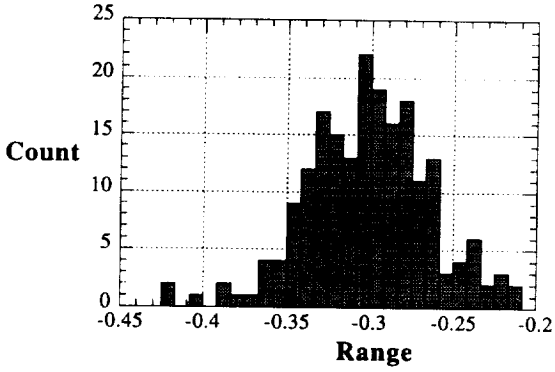

Figure 3 C_{M_α} estimates from Monte Carlo simulation

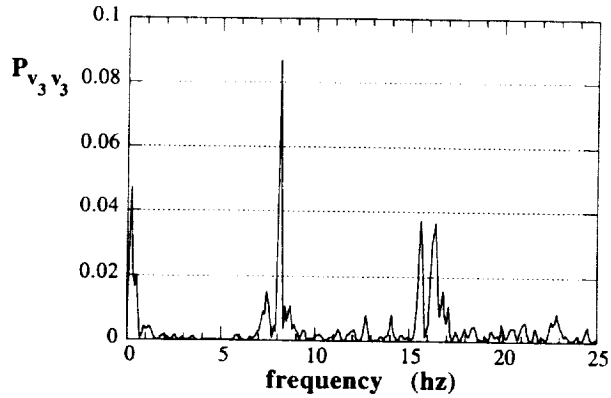

Figure 4 Power spectrum of a_z residuals, flight test run 1

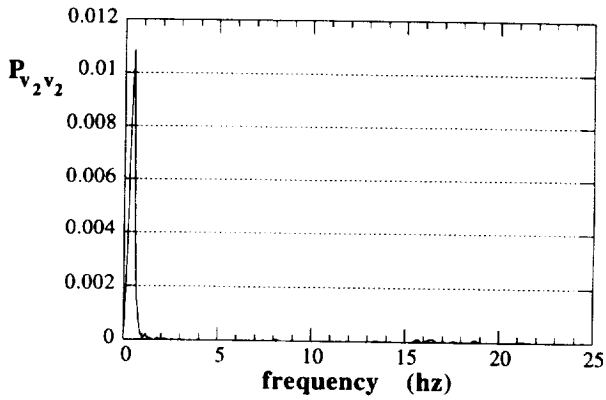

Figure 5 Power spectrum of q residuals, flight test run 1

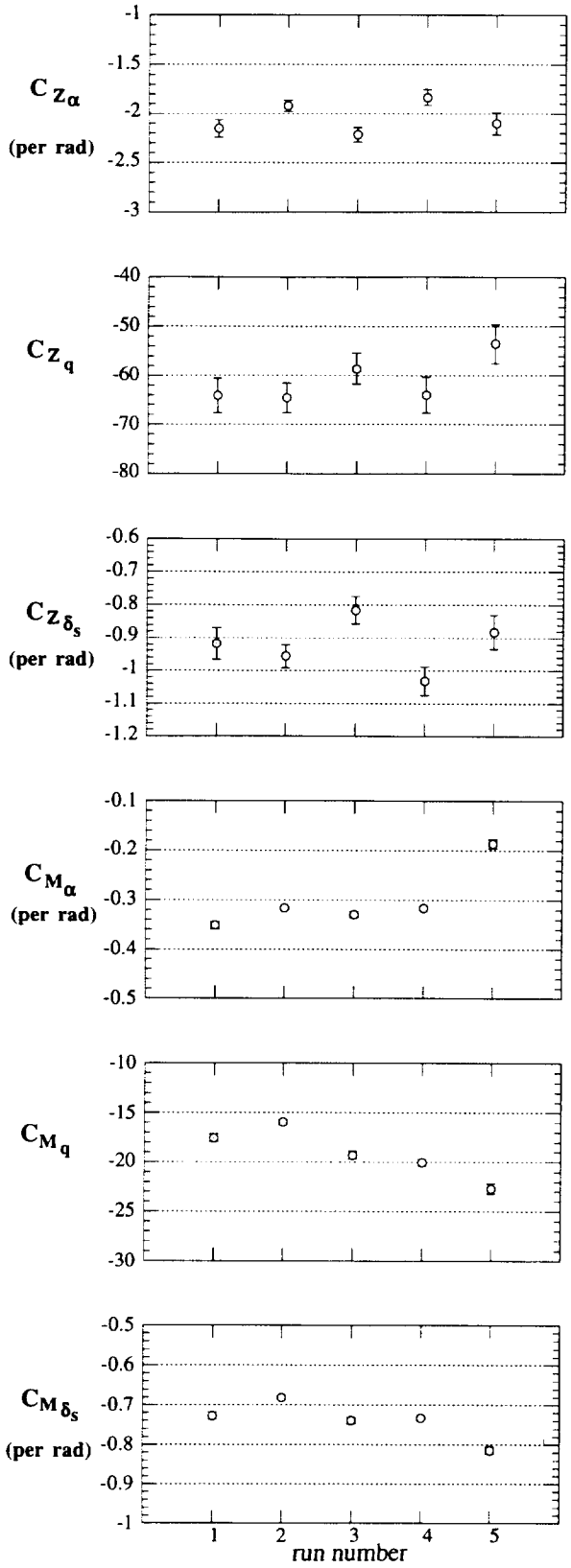

Figure 6 Parameter estimates with conventional error bounds

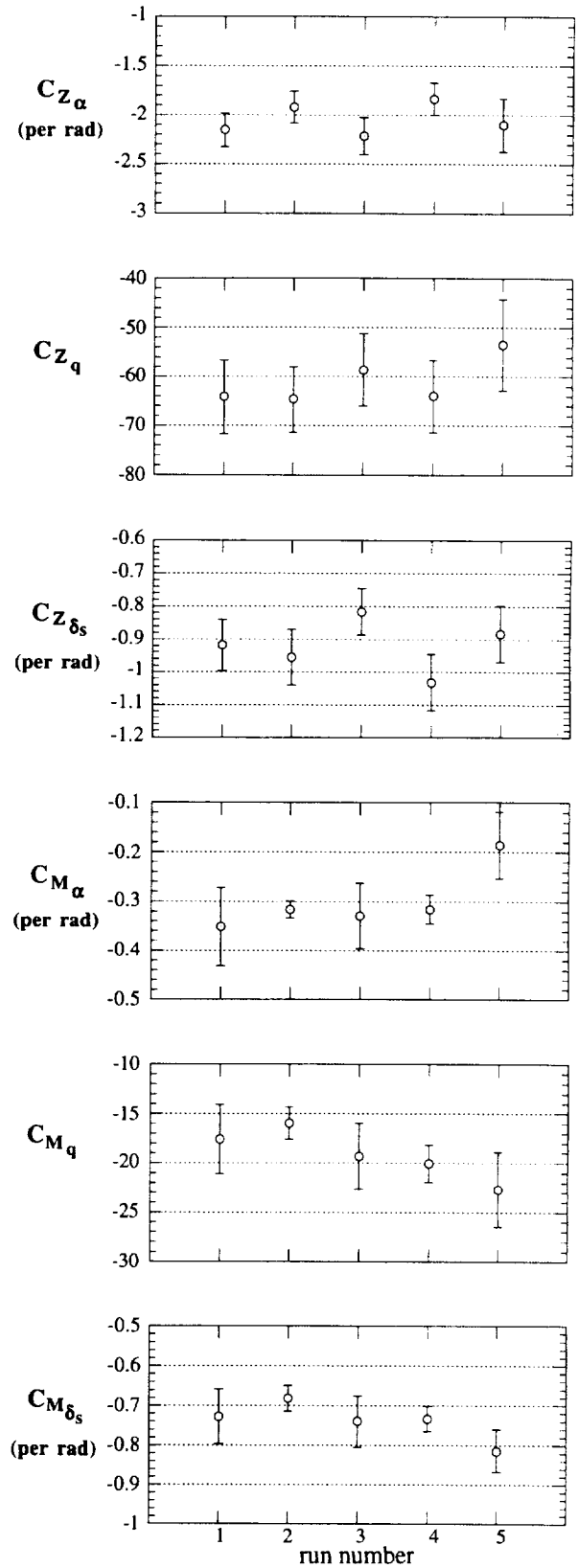

Figure 7 Parameter estimates with corrected error bounds